ISSN 1392 - 1207. MECHANIKA. 2012 Volume 18(6): 705-712

Elaboration of analytical thermo-mechanical cutting model matched by numerical and experimental results

F. Salvatore*, T. Mabrouki, H. Hamdi*****
**Université de Lyon, ENISE, LTDS, UMR 5513 CNRS, 58 rue Jean Parot, 42023 Saint Etienne, France,*
E-mail: ferdi3@free.fr
***Université de Lyon, INSA Lyon, LAMCOS, UMR 5259 CNRS, 18-20 rue des Sciences, 69621 Villeurbanne, France,*
E-mail: Tarek.Mabrouki@insa-lyon.fr
****Université de Lyon, ENISE, LTDS, UMR 5513 CNRS, 58 rue Jean Parot, 42023 Saint Etienne, France,*
E-mail: hamdi@enise.fr

crossref http://dx.doi.org/10.5755/j01.mech.18.6.3161

1. Introduction

Cutting processes are widely used in different industries to cut various engineering parts. Usually the optimization of these processes is made by experimental methods often expensive and not able to be extrapolated to other machining configurations. To overcome these drawbacks, numerical simulations have been carried out by many researchers but the major inconvenience of those methods are the long computing time, the high cost of numerical software, etc. For all these reasons, in manufacturing industry, a high interest in analytical methods such as that of Merchant [1, 2] and Lee and Schaffer [3] are usually adopted because they are practical and simple to use. Other authors such as Gilormini, Molinari, Moufki, and Oxley [4-8] have proposed pertinent thermo-mechanical cutting models but not convenient to use and not taking into account the cutting radius influence, ploughing and the spring back.

For all those reasons the present work is both complete and predictive in order to be really interesting compared to experimental and numerical methods.

It is based on a new "phenomena split approach" (PS-approach) (Fig. 1) which can be directly and efficiently exploited also from practical point of view.

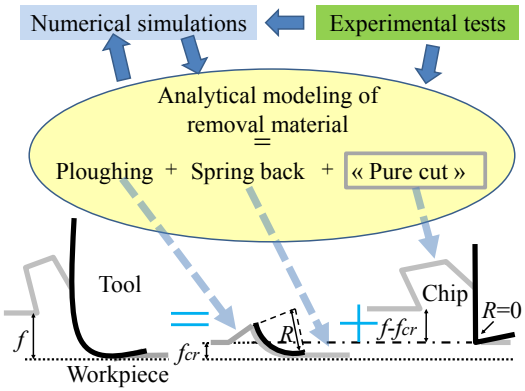

Fig. 1 Schematization of the cutting process with the "phenomena split approach"

This methodology stems from experimental observations in the case of turning. In fact, burrs appear during the cutting process for different manufacturing input parameters or when a threshold of tool wears is reached. Burr is the result of a plastic flow of material similar to ploughing observed in scratch tests [9-11].

Consequently, it is assumed (Fig. 1) that a cutting phenomenon can be decomposed as a sum of three elementary phenomena: pure cutting, ploughing and spring back, where R is the tool cutting radius, f is the uncut chip thickness, f_{cr} is the critical feed rate characterizing the limit value between ploughing and "pure cut" (i.e. chip formation).

The proposed analytical model of the chip formation is performed using the mechanical balance formulation [1, 2] and the assumption that the shear zones thickness, where deformations are considered concentrated, are constants [8] but the calculation of the temperature in those zones are a function of different partition heat coefficients.

Others new hypothesis and equations are introduced by the use of FEM studies, in particular, stresses and forces distributions, triaxiality close to the tip of the tool.

Those numerical contributions substitutes the equations based on the minimization of the cutting energy like acted by Merchant and Gilormini [1, 2, 4].

The influence of tool geometry in terms of chip formation is also studied and an equivalent cutting angle is introduced to replace the cutting radius. In this way the rake face stay plane and, the forces and temperature formulations are simpler than those proposed by Albrecht [12] and "linked" to the thermo-mechanical approach.

First experimental tests, materials employed and the measured data such as forces and chip thickness are presented. Then a cutting numerical simulation based on ABAQUS Explicit is developed in order to identify more accurately the influences of physical phenomena. Afterwards the general PS-approach assumptions are presented but only the "pure cut" contribution is described in detail. Finally, the most important results of the sub-model "pure cut" are presented, discussed and compared to Merchant.

2. Experimental study

In this section the experimental cutting tests are presented. In order to replicate orthogonal cutting conditions, the machining operation was carried out on discs each one with a diameter of 70 mm and a thickness (a_p) of 3 mm, which is also the cutting depth.

The cutting tool is in a carbide grade (referenced TPKN 16 03 PP R SM30) with cutting edge radius R of 30 μm. The machined material is a steel alloy AISI 4140.

The values of a_p and R were chosen to minimize ploughing effects (lateral burrs). In fact in this paper the

adopted "PS approach" is presented, but only the elementary model "pure cut" is adopted, verified and fitted with experimental and numerical methods. For that, in the next the value of f_{cr} is considered equal to zero.

Cutting speed variations were made in order to measure machining forces using a dynamometer Kistler 9257 A with a sampling frequency about 2 KHz (Fig. 2).

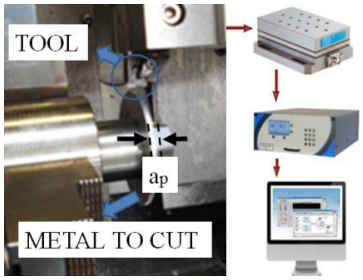

Fig. 2 Experimental test procedure

Details of the averages of cutting forces F_x, feed forces F_y, and primary shear angle Φ are presented in Table 1 and 2 in the section "analytical results and discussion", compared to numerical and analytical data.

3. Numerical study

Numerical simulations based on Abaqus\Explicit (Lagrangian formulation) were performed in order to both understand the physics of cutting and improve the analytical method. The Johnson and Cook's law [13] is used for the workpiece material behaviour.

The workpiece is geometrically modelled according to Mabrouki [14]. Parameters of the tool and the workpiece are extracted from Barge study [15] and the material to cut is characterized with also the Johnson and Cook damage law [16].

From contact point of view, the "surface to surface" interaction option and the penalty contact method were chosen. Also, it is considered that $\mu = 0.39$ for $V_c = 42$ m/min, $\mu = 0.30$ for $V_c = 126$ m/min, $\mu = 0.25$ for $V_c = 378$ m/min according to experimental results of Zemzemi [17].

In order to find the good mesh dimensions for the numerical simulations, the influence of the primary shear zone thickness d_1 versus the cutting speed V_c for different vertical mesh sizes was made (Fig. 3).

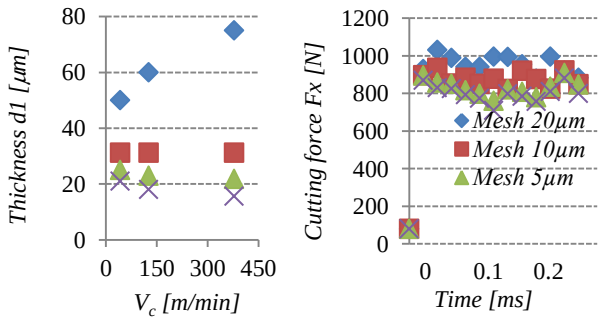

Fig. 3 Numerical thickness d_1 and cutting force F_x in case of AISI 4140 steel, $f = 0.15$ mm, $\gamma = 0$, $\mu = 0$

In this specified study frictionless assumption was adopted for the chip-tool contact. The cutting angle γ was considered equal to zero.

From this last figure, it is possible to underline that smaller the mesh size values, smaller the primary shear zone thickness. This is due to the strain localization phenomenon which induces high temperature (Fig. 4). The material softening induces lower forces and, by the same way, lower thickness of the primary shear zone.

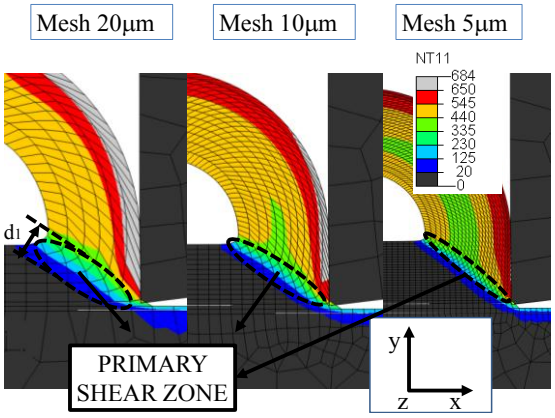

Fig. 4 Nodal temperature (NT11) output [°C] in case of $f = 0.15$ mm, $R = 0$, $\mu = 0$, $\gamma = 0$. Mesh size from 5 to 20 µm and $V_c = 378$ m/min

The computed primary shear zone thickness for a mesh size varying from 5 to 10 µm is close to the value (25 µm) given by Shaw [18].

Consequently 10 µm mesh size is adopted in this study and seems in agreement with Barge [15].

Using a 10 µm mesh dimension and the previous friction coefficient, it is then possible to perform numerical simulation and compare results to experimental and analytical cutting forces (Fig. 5) and primary shear angle Φ, (Table 1 and 2).

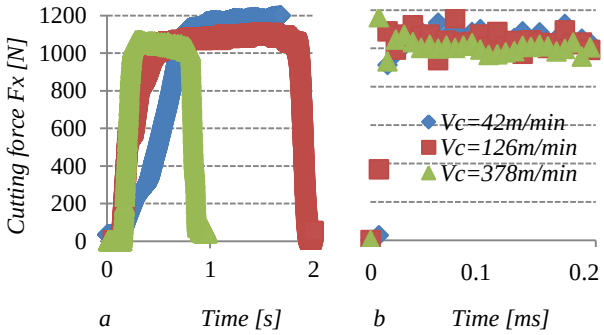

Fig. 5 Measured forces (a) and computed one's with FE (b) versus time in the case of a mesh 10×10 µm for different cutting speeds, $f = 0.15$ mm and $\gamma = 0$

In the presented FE simulations the deformation is supposed to be uniform. This assumption is justified by the manner of the calculation of the primary shear angle as a function of feed rate divided by chip thickness.

For the different outputs presented, numerical results are in concordance with the experimental ones. It is then considered that the present numerical model reproduces the real phenomena and will be used to calibrate further analytical cutting modelling.

In order to have numerical simulations without the influence of the friction coefficient, the principal out-

puts using the "frictionless" option in the contact between the tool and chip are now studied. The cutting radius is considered null and f_{cr} too.

It is decided to chose four chip sections (Fig. 6). Primary shear zone is delimited by section *1* and *3*. Section *4* is the "interface" between tool and chip.

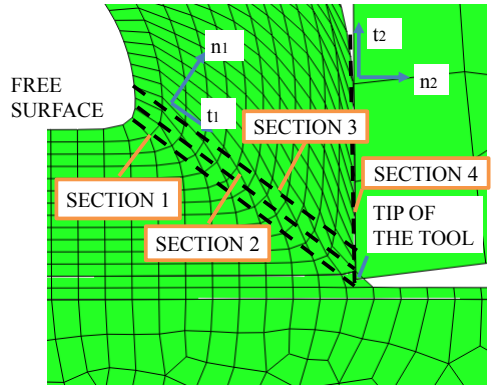

Fig. 6 Different sections employed in numerical simulations

In Fig. 7 to 9, the normal and tangential stresses distributions in the primary shear zone and the normal distribution in the secondary one are presented in the case of f = 0.15 mm, R = 0, γ = 0, μ = 0.

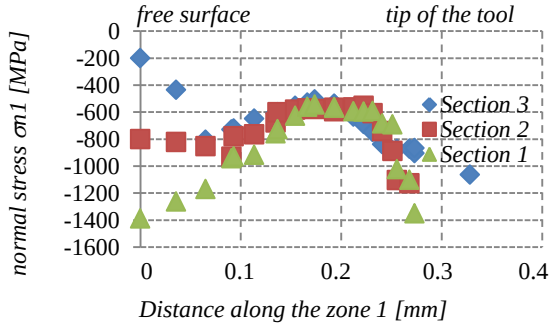

Fig. 7 Normal stress σ_{n1} in the primary shear zone from the free surface (distance = 0) to the tool tip (distance = 0.27 mm)

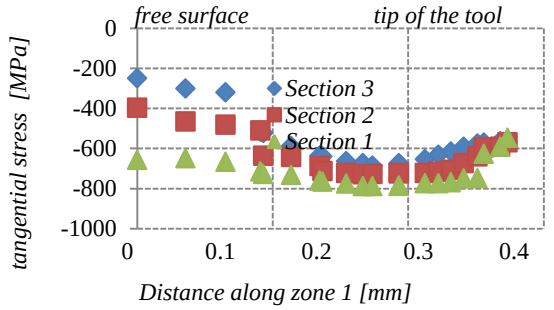

Fig. 8 Tangential stress τ_1 is investigated from the free surface to the tool tip

In Fig. 7, σ_{n1} distribution is similar in every chosen section inside the primary shear zone, close to the tool. In this zone the triaxiality is high. In the primary shear zone region close to the free surface, it is possible to capture the opposite situation; along section *1* the stress value is the bigger and along section *3* it is close to zero. In fact, in this last section, and close to the free surface, the chip is still formed and the effects of the compression in zone *2* are far. Consequently it is acted that the plastic strain can be considered concentrated in the shear zones. This hypothesis will be done in the analytical section and is in accordance with [5-8].

In the same way, the tangential stress distribution in the primary shear zone (Fig. 8) is quite similar in every chosen section close to the tool.

In this case it is decided to formalize the uniform distribution for the analytical modeling.

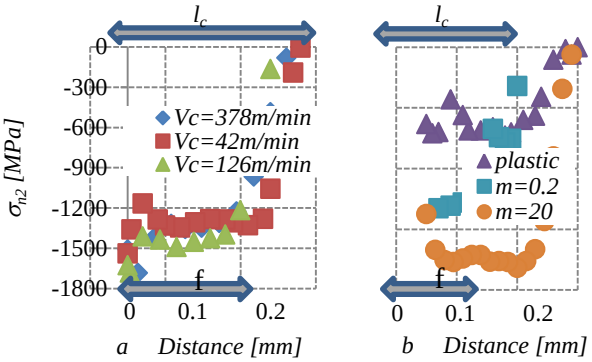

Fig. 9 Normal stress σ_{n2} in zone *2* (section *4*). a - different cutting speed using the adopted behavior law; b - the "pure plastic" case is presented and 2 different values of the m exponent in Johnson and Cook law in the case 378 m/min

In Fig. 9, the normal stress distribution in the region of the chip close to the tool is represented (section *4*). For every condition there is a uniform part from the tip of the tool to the "*f*" value and, from *f* to the contact length l_c, the distribution became triangular. This is verified for three cutting speeds and, for different Johnson and Cook parameters, in the case of V_c = 378 m/min.

Afterwards, the forces distribution hypothesis, acted in Fig. 10, are validated in this section.

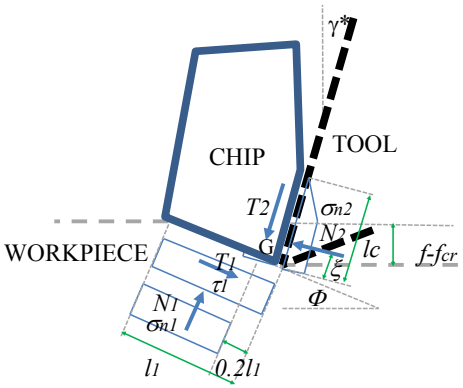

Fig. 10 Stresses and forces distributions applied to the chip

Afterwards the triaxiality is big in the region of the piece close to the tip of the tool. The normal stress value in the primary shear zone is close to the normal stress value in the interface tool-chip (Figs. 7-9).

From those considerations it is possible to extract new simple Eqs. (1) and (2) where the maximum value of the normal stress σ_{n2max} is a function of the tangential one τ_1. The normal force N_2 in the secondary shear zone is a function of τ_1.

$$\sigma_{n1max} = \sigma_{n1max} = \sqrt{3}\tau_1 \quad (1)$$

$$N_2 = a_p \int_0^{l_c} \sigma_{n2} dl = \frac{\sqrt{3}}{2} a_p \tau_1 \left[l_c + \frac{f - f_{cr}}{\cos(\gamma^*)} \right] \quad (2)$$

where γ^* is the equivalent cutting angle explained in the next section. Eqs. (1) and (2) are verified for different Johnson and Cook parameters (Fig. 9). For those reasons it is considered that it can be applied for different types of materials.

4. Cutting analytical model

4.1. Introduction

Orthogonal cutting represented by a 2D model is considered in the present study. The cutting tool removes a specific layer of work material (Fig. 11). f is the theoretical uncut thicknesses to remove with the tool, R is the cutting edge radius, f - f_{cr} the real layer of work material removed. In fact for low values of the f/R ratio ($f < f_{cr}$) the chip formation does not occur; only spring back and ploughing appear (in case of 3D approach). The chip formation is only possible if f is greater than f_{cr}: in this case it is supposed that the cutting process is made with a virtual tool, with a cutting edge radius $R = 0$ (Fig. 11), and the effective layer work material removed is f - f_{cr}.

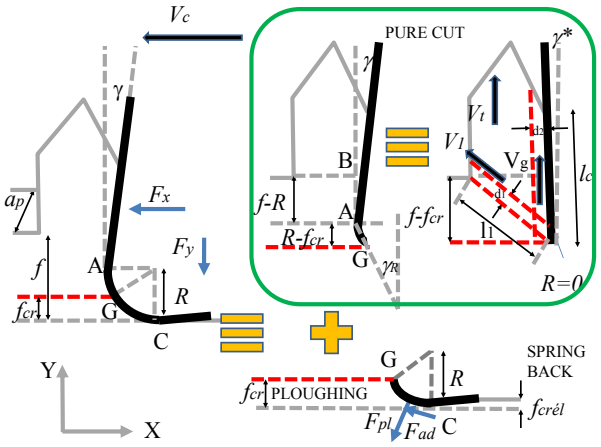

Fig. 11 Schematization of the "PS- approach". Forces, geometrical variables and the equivalent cutting angle γ^* are presented

f_{cr} gives the supposed position of the separation line between the material that will became chip and the part of metal that will slide under the tool (spring back) or will be displaced laterally (ploughing).

The ploughing and spring back phenomena are concentrated in the layer defined from the point C to the point G.

It is also supposed that the ploughing and spring back variables only depend on f_{cr} value. It will thus be possible to apply the effect superposition principle and study separately all those phenomena.

In the proposed approach the ploughing and spring back phenomena are caused by the cutting radius and, if it is zero, only the pure cutting condition will exist.

Moreover the effects of the cutting radius exists in "pure cutting case" too; it will be explained in the next section.

4.2. Modeling of cutting radius contribution

The cutting radius contribution must be taken into account when sliding and normal forces on the tool rake face are considered. Both cutting radius and rake face are modeled by a single equivalent rake face without cutting radius ($R = 0$) and consequently with an equivalent cutting angle γ^* (Fig. 11).

The latter angle is the summation of 2 contributions. The first one is the local cutting angle caused by the cutting radius; its action is localized in the layer "R - f_{cr}" (AG).

The second one is the contribution of the angle γ in the "f - R" layer (AB).

It is remembered that the part "CG" of the cutting edge R is the ploughing contribution not presented in this paper.

Based on geometrical considerations the equivalent cutting angle γ^* is given by equation

$$\gamma^* = -\left(\frac{R - f_{cr}}{f - f_{cr}} \right) arctan\left(\frac{R - \sqrt{2Rf_{cr} - f_{cr}^2}}{R - f_{cr}} \right) + \left(\frac{f - R}{f - f_{cr}} \right) \gamma \quad (3)$$

It is noted that, when the ratio f/R is very big, γ^* is close to γ. In the opposite situation, when f/R is close to 1 γ^* is similar to γ_R.

Having now the calculation of the equivalent cutting angle it is possible to compute forces F_x and F_y.

Based on the ploughing F_{pl} and friction force F_{ad} in the layer defined by "CG", and, according to Fig. 11 the cutting and feed force can be presented respectively by Eqs. (4) and (5).

$$F_x = T_2 \sin(\gamma^*) + N_2 \cos(\gamma^*) + F_{ad}\big|_x + F_{pl}\big|_x \quad (4)$$

$$F_y = T_2 \cos(\gamma^*) - N_2 \sin(\gamma^*) - F_{ad}\big|_y + F_{pl}\big|_y \quad (5)$$

where N_2 is the orthogonal force on the tool rake face, T_2 is the tangential or friction force, T_1 and N_1 are the tangential and normal forces in the primary shear zone, respectively.

All those last variables are to be computed, as what it is suggested in section 4.3.

In the "pure cutting case" F_{ad} and F_{pl} are considered equals to zero.

4.3. Pure cutting case

Pure cutting involves $f > f_{cr}$. Chip formation is made using an "equivalent" tool with a cutting radius $R = 0$, a cutting equivalent angle γ^* (Eq. (3)), and the layer of material removed is f - f_{cr}.

The chip is assumed rigid and uniform except in zone *1* and *2* where all the deformations are localized [5-8]. This last assumption is in concordance with the results given by FE cutting model. The thicknesses of these zones are d_1 and d_2. In both zones, the assumption of thermo-viscous-plastic-hardening material behaviour is made [13].

According to Fig. 10 and when applying the force

equilibrium conditions on the chip (forces and momentum), it is possible to write Eqs. (6)-(8).

$$N_1 \sin(\Phi) + T_1 \cos(\Phi) = T_2 \sin(\gamma^*) + N_2 \cos(\gamma^*) \quad (6)$$

$$-T_1 \sin(\Phi) + N_1 \cos(\Phi) = -N_2 \sin(\gamma^*) + T_2 \cos(\gamma^*) \quad (7)$$

$$N_1 \frac{0.6(f - f_{cr})}{\sin(\Phi)} = N_2 \xi l \quad (8)$$

ξ is the distance between the tip of the tool and the point where the force N_2 is applied. This variable can be computed using Eqs. (1) and (2) in Eq. (8).

From Eq. (6) it will be possible to extract N_1, from Eq. (7) the shear angle Φ and from Eq. (8) the contact length l_c.

σ_{n2max} and N_2 can be computed with Eqs. (1) and (2). Forces and stresses distribution are in accordance with Fig. 10.

By applying the Johnson and Cook law (Eq. (9)) in the zone *1*, the tangential force T_1 can be calculated by Eq. (11). In this case the tangential stress τ_1 calculation is proposed in shear formulation.

$$\tau_1 = \left[\frac{A}{\sqrt{3}} + \frac{B\gamma_{d1}^n}{\sqrt{3}^{n+1}}\right]\left[1 + CLn\left(\frac{\dot{\gamma}_{d1}}{\dot{\gamma}_{d0}}\right)\right] \times \times \left[1 - \left(\frac{T_{emp1} - T_{emp0}}{T_{melt} - T_{emp0}}\right)^m\right] \quad (9)$$

$$T_1 = a_p \int_0^{l_1} \tau_1 dl_1 = a_p \tau_1 l_1 = \frac{a_p \tau_1 (f - f_{cr})}{\sin(\Phi)} \quad (10)$$

where l_1 is the length of the primary shear zone, *A*, *B*, *n*, *C*, *m* and are Johnson and Cook parameters.

The unknown parameters in Eq. (9) are now computed; in particular the strain is given by Eq. (11) and the strain rate by Eq. (12).

$$\gamma_{d1} = \frac{1}{\tan(\gamma^* + \pi/2 - \Phi)} + \frac{1}{\tan(\Phi)} \quad (11)$$

$$\dot{\gamma}_{d1} = \frac{V_1}{d_1} \quad \text{with} \quad V_1 = \frac{V_c}{\cos(\Phi) + \sin(\Phi)\tan(\gamma^*)} \quad (12)$$

In Eqs. (11) and (12), d_1 and V_1 are, respectively, the thickness and the shearing speed along l_1 in the primary shear zone. The first of those equations is similar to Moufki [7] and it can be considered a generalised version because it takes into account the cutting radius *R* with the equivalent cutting angle γ^*.

Now, in order to compute the temperature T_{emp1} in the primary shear zone, it is considered that the force T_1 produce the work Q_1 to shear the primary zone with a strain done by equation l_1. It is also considered that 90% of this work became heat and this last variable is multiplied by a partition heat coefficient to take into account the part of heat that is conduced into the workpiece. Afterwards the volume where the heat is generated is defined by d_1, l_1 and a_p (Fig. 11).

Consequently it is possible to compute equation

$$T_{emp1} = T_{emp10} + (1 - \delta_1)\frac{0.9\gamma_{d1}\tau_1}{C_p \rho} \quad (13)$$

In order to have a low sensibility of d_1 in the case of very negatives angles (γ^*) computed values, it is decided to use Eq. (14). It is still close to Oxley estimation [8] where d_1 is equal to 10% of the primary shear zone length.

$$d_1 = 0.2(f - f_{cr}) \quad (14)$$

In Eq. (13), δ_1 is the heat partition coefficient between the chip and the workpiece and T_{emp10} is the initial temperature in the primary shear zone, equals to the initial temperature of the workpiece. In this paper the method of Gilormini [4] to compute δ_1 is adopted

$$\delta_1 = \frac{\cot an(\Phi) k_2}{\rho C_p V_c (f - f_{cr})}\left[1 - exp\left(-\frac{\rho C_p V_c (f - f_{cr})}{\cot an(\Phi) k_2}\right)\right] \quad (15)$$

where k_2 and C_p are, respectively, the conductivity and the specific heat of the workpiece.

The last variable to be computed to solve the system is the friction force at the interface tool-chip T_2.

It is supposed a sticky contact from the point B to G and a sliding contact from B to C. This is based on numerical simulations (Fig. 9) where from the point B to G the normal stress is constant and from B to C it degrease to zero.

In the present work the partition of the secondary shear zone is similar to the Bahi works [19] where the sticking and sliding contact is defined and based on the measurement of the friction coefficient. In our case the approach is more easy and predictive.

It is also supposed that the thickness of the secondary shear zone d_2 is equal to d_1.

Consequently, the strain and the strain rate are given by the following equations, respectively

$$\gamma_{d2s} = \frac{f - f_{cr}}{\cos(\gamma^*) d_2} \quad (16)$$

$$\dot{\gamma}_{d2s} = \frac{V_t}{d_2} = \frac{V_c \sin(\Phi)}{\cos(\Phi - \gamma^*) d_2} \quad (17)$$

In the same way as it was computed T_{emp1}, it is now suggested the temperature $\Delta T'_{emp2s}$ generated in the sticky zone in the secondary shear zone (Eq. (18)).

$$\Delta T'_{emp2s} = (1 - \delta_{2s})\frac{Q_{2s}}{\rho W_{2s} C_p} = (1 - \delta_{2s})\frac{0.9\gamma_{d2s}\tau_{2s}}{\rho C_p} \quad (18)$$

δ_{2s} is heat partition coefficient between the tool and the workpiece computed with Jaeger method [20] in the case of sticky contact, as shown in equation

$$\delta_{2s} = \frac{k_1}{k_1 + k_2\sqrt{\frac{0.5(f - f_{cr})V_t}{\cos(\gamma^*)\alpha_2}}} \quad (19)$$

where k_1 and k_2 are the conductivities of the tool and the

workpiece, respectively. α_2 is the diffusivity of the steel.

τ_{2s} in Eq. (18) is the tangential sticky shear stress in zone *2* computed with Johnson and Cook law (Eq. (20)).

$$\tau_{2s} = \left[\frac{A}{\sqrt{3}} + \frac{B\gamma_{d2s}^{n}}{\sqrt{3}^{n+1}}\right]\left[1 + CLn\left(\frac{\dot{\gamma}_{d2s}}{\dot{\gamma}_{d0}}\right)\right] \times \left[1 - \left(\frac{T_{emp2s} - T_{emp0}}{T_{melt} - T_{emp0}}\right)^{m}\right] \quad (20)$$

T_{emp2s} is the temperature in this sub zone (sticky). It is the summation of the temperature of the zone *1*, displaced to the secondary shear zone during the chip evolution, and $\Delta T'_{emp2s}$.

Consequently it is possible to write

$$T_{emp2s} = (1-\delta_1)\frac{0.9\gamma_{d1}\tau_1}{\rho C_p} + (1-\delta_{2s})\frac{0.9\gamma_{d2s}\tau_{2s}}{\rho C_p} \quad (21)$$

In the zone BC, a sticky-sliding contact is assumed. Here the strain and the strain rate are not constants like considered in the sticky zone. In fact it is supposed that in the point B the contact is still sticky ($V_g = 0$) and in the point C totally sliding ($V_g = V_t$). In order to easy compute variables of this zone, an only sticky contact is supposed in half distance BC. In the other half distance a totally sliding contact is considered ($\mu = 0$). Consequently

$$\gamma_{d2g} = \frac{1}{2d_2}\left(l_c - \frac{f - f_{cr}}{\cos(\gamma^*)}\right) \quad (22)$$

$$\dot{\gamma}_{d2g} = \frac{V_t}{\cos(\gamma^*)d_2} = \frac{V_c \sin(\Phi)}{\cos(\Phi - \gamma^*)\cos(\gamma^*)d_2} \quad (23)$$

The temperature generated by heat $\Delta T'_{emp2g}$ is presented in equation

$$\Delta T'_{emp2g} = (1-\delta_{2g})\frac{Q_{2g}}{\rho W_{2g} C_p} = (1-\delta_{2g})\frac{0.9\gamma_{d2g}\tau_{2g}}{\rho C_p} \quad (24)$$

where, δ_{2g} and τ_{2g} are computed with Jaeger and Johnson and Cook formulations, respectively (Eqs. (25) and (26)).

$$\delta_{2g} = \frac{k_1}{k_1 + k_2\sqrt{\frac{0.5\left[l_c - (f - f_{cr})/\cos(\gamma^*)\right]V_t}{\alpha_2}}} \quad (25)$$

$$\tau_{2g} = \left[\frac{A}{\sqrt{3}} + \frac{B\gamma_{d2g}^{n}}{\sqrt{3}^{n+1}}\right]\left[1 + CLn\left(\frac{\dot{\gamma}_{d2g}}{\dot{\gamma}_{d0}}\right)\right] \times \left[1 - \left(\frac{T_{emp2g} - T_{emp0}}{T_{melt} - T_{emp0}}\right)^{m}\right] \quad (26)$$

T_{emp2g} is done by Eq. (27), where T_{emp2s} is the "initial" temperature of this sub-zone, because of the displacement of the chip. T_2 is resolved using Eq. (28).

$$T_{emp2g} = T_{emp2s} + (1-\delta_{2g})\frac{0.9\gamma_{d2g}\tau_{2g}}{\rho C_p} \quad (27)$$

$$T_2 = \tau_{2s}\frac{f - f_{cr}}{\cos(\gamma^*)}a_p + \frac{\tau_{2g}}{2}\left(l_c - \frac{f - f_{cr}}{\cos(\gamma^*)}\right)a_p \quad (28)$$

Now it can be allowable to compute the friction coefficient in the interface between the tool and the chip as the ratio between T_2 and N_2.

4.4. Analytical results and discussions

According to Fig. 11, the most important variables of the study are resumed in Table 1 and 2, compared to numerical and experimental results.

The values of analytical forces and temperatures presented in Tables 1 and 2 are similar to experimental [21] and numerical ones. Concerning the primary shear zone angle Φ, the analytical calculation is accurate for cutting speeds major than 126 m/min if f is bigger than 0.15 mm.

In the case of feed rate equal to 0.07 mm, it appears that, for low cutting speed (42 m/min) the analytical calculation of Φ is accurate; this is due to the equivalent cutting angle γ* equal to -0.33 rad. Feed force F_y is also close to experimental data.

The presented "pure cut" sub-model is based on a thermo-mechanical approach using Johnson and Cook's law in the shear zones *1* and *2*. Stresses value in those zones are a function of the shear strain, shear strain rate and temperature. The firsts one are function of the equiva-

Table 1

Analytical, experimental and numerical results in case of AISI 4140 steel, carbide tool, f = 0.15 mm, γ^* = -0.15 rad. In brackets Merchant [1, 2] calculation

V_c, m/min	Computing method	Cutting force F_x, N	Feed force F_y, N	Primary shear angle Φ, Rad	Contact length/feed, l_c/f	T_{emp1}, °C (zone *1*)	$T_{em2s,}$ °C (zone *2* sticky)	$T_{em2g,}$ °C (zone *2* sliding)
42	Analytical	1056 (1447)	611 (434)	0.58 (0.45)	3.02 (2.12)	432	885	1048
	Experimental	1118	563	0.45				
	Numerical	1150	556	0.48	2.41	451	931	1024
126	Analytical	981 (826)	512 (207)	0.61 (0.58)	2.81 (1.7)	485	960	1130
	Experimental	1052	495	0.58				
	Numerical	1102	457	0.57	2.31	495	991	1051
378	Analytical	949 (699)	474 (140)	0.62 (0.60)	2.74 (1.57)	509	1006	1171
	Experimental	998	412	0.6				
	Numerical	982	393	0.58	2.19	521	1021	1146

Table 2

Analytical and experimental results in case of AISI 4140 steel, carbide tool, f = 0.15 mm, γ^* = -0.15 rad

Feed f, mm/rev	Computing method	Cutting force F_x, N	Feed force F_y, N	Primary shear angle Φ, Rad	Contact length/feed l_c/f	Temperature zone *1* T_{emp1}, °C	Temperature zone 2 T_{emp2s},°C	Temperature zone 2 T_{emp2g}, °C
0.07	Analytical	554	311	0.51	3.81	375	830	1001
	Experimental	512	304	0.44				
0.225	Analytical	1459	741	0.62	2.75	439	960	1129
	Experimental	1552	798	0.49				

lent cutting angle γ^* and, consequently the cutting radius R. The temperatures are function of the strains but also of the heat partition coefficients. In particular those last variables depend on the diffusivity of the material and the cutting parameters f and V_c.

For low values of f and V_c the heat partition coefficients δ_1 are close to 1 and for high values of those "machining parameters" it is close to 0. This leads to low temperatures and high forces because the "softening" contribution in Johnson and Cook equations became small.

Finally, concerning the comparative with Merchant calculation, it is possible to act (Table 1) that the precision in terms of F_x and F_y is lower than the proposed "pure cut" model. Only the angle Φ is more accurate here because it is the "set parameter". F_y values are smalls because the cutting radius effect is not taken into account.

5. Conclusions

In this paper an analytical model of material removal is presented. This model is based on the new assumption that cutting operation can be defined as a sum of three contributions: ploughing, spring back and pure cut.

It was decided to present and study in details the "pure cut" sub-model where the chip formation is investigated. In this case the analytical model was fitted with FEM simulations and verified with experimental tests.

In particular the stresses distribution is numerically studied and the outputs of this investigation were acted in new formulations based on triaxiality and forces distributions applied to the chip.

In the sub-model "pure cut", the chip is considerate rigid and the static equilibrium of the chip leads to the definition of three simple equations like Merchant [1, 2]. The thermo-mechanical assumption was made in the shear zones 1 and 2 where the strain is supposed to be concentrated [5-8].

The temperature calculation is made using the definition of specific heat in the shear zones.

The cutting radius of the tool is modelled using an equivalent cutting angle what is new compared to the precited works. The ratio f/R is important and define 2 different conditions. If it is big the cutting radius R can be considered null, but if it is low, it is necessary to model the radius R. It is the industrial case of damaged tools.

The calculations of the variables of the model are only functions of input parameters (process parameters and thermo-mechanical data) and no experimental setting like chip thickness measurements are required.

The analytical equations can be directly used for industrial application or for scientific purpose, in order to have easier data to understand the removal material problem before a more intense research.

The proposed analytical model can be employed for several steels if parameters of Johnson and Cook law exist.

"PS approach" can be exploited to predict residual stresses after machining, where the cutting radius and the ploughing are important for the accuracy of the study.

References

1. **Merchant, M.E.** 1945. Mechanics of the metal cutting process. I. Orthogonal cutting and a type 2 chip, Journal of Applied Physics (USA), American Institute of Physics, 267-275.
2. **Merchant, M.E.** 1945. Mechanics of the metal cutting process. II. Plasticity conditions in Orthogonal cutting, Journal of Applied Physics (USA), American Institute of Physics, 267-275.
3. **Lee, E.H.; Shaffer, B.** 1951. The theory of plasticity applied to problems of machining, Journal of Applied Mechanics, Américan Society of Mechanical Enginneers, 405-413.
4. **Gilormini, P.; Felder, E.** 1985. Modelisation thermomécanique de la formation du copeau en usinage à grande vitesse, Bulletin du Cercle des Métaux 15-9.
5. **Molinari, A.** 2004. A new thermomecanical model of cutting applied to turning operations Part 1 Theory, int J. Mach. Tools Manufacture 45: 166-180. http://dx.doi.org/10.1016/j.ijmachtools.2004.07.004.
6. **Moufki, A.; Devillez, A.; Dudzinski, D.; Molinari, A.** 2002. Thermo mechanical modeling of cutting and experimental validation, Metal Cutting and High Speed Machining, 51-67.
7. **Moufki, A.; Molinari, A.; Dudzinski, D**. 1998. Modelling of orthogonal cutting with a temperature dependent friction law, J. Mech. Phys. Solids 46: 2103-2138. http://dx.doi.org/10.1016/S0022-5096(98)00032-5.
8. **Oxley, P.L.B**. 1989. Mechanics of Machining: An Analytical Approach to Assessing Machinability, Ellis Horwood limited, Chichester.
9. **Ben Tkaya, M.; Zahouani, H.; Mezlini, S.; Kapsa, Ph.; Zidi, M.; Dogui, A.** 2007. The effect of damage in the numerical simulation of a scratch test, Wear 263: 1533-1539. http://dx.doi.org/10.1016/j.wear.2007.01.083.
10. **Felder, E.; Bucaille, J.L.** 2006. Mechanical analysis of the scratching of metals and polymers with conical indenters at moderate and large strains, Tribology International 39: 70-87. http://dx.doi.org/10.1016/j.triboint.2005.04.005.
11. **Jardret, V.; Zahouani, H.; Lobet, J.L.; Mathia, T.G.** 1998. Understanding and quantification of elastic and plastic deformation, Wear 218(1): 8-14. http://dx.doi.org/10.1016/S0043-1648(98)00200-2.
12. **Albrecht, P.** 1960. New developpements in the theory

of the metal cutting processes - Part I: The ploughing process in the metal cutting, Journal of Engineering for Industry Transactions of ASME, 82: 348-362. http://dx.doi.org/10.1115/1.3664242.
13. **Johnson, G.R.; Cook, W.H.** 1983. A constitutive model and data for metals subjected to large strains, strain rates and high temperatures, 7th Int. Symp. Ballistics, 541-547.
14. **Mabrouki, T.; Rigal, J.F.** 2006. A contribution to a qualitative understanding of thermo-mechanical effects during chip formation in hard turning, Journal of Material Processing Technology, 176: 214-221. http://dx.doi.org/10.1016/j.jmatprotec.2006.03.159.
15. **Barge, M.; Hamdi, H.; Rech, J.; Bergheau, J.M.** 2005. Numerical modelling of orthogonal cutting: influence of numerical parameters, Journal of Materials Processing Technology, 164-165: 1148-1153. http://dx.doi.org/10.1016/j.jmatprotec.2005.02.118.
16. **Johnson, G.R.; Cook, W.H.** 1985. Fracture characteristics of three metals subjected to various strains, strain rates, temperatures and pressures, Engineering Fracture Mechanics 21: 31-48. http://dx.doi.org/10.1016/0013-7944(85)90052-9.
17. **Zemzemi, F.; Rech, J.; Ben Salem, W.; Dogui, A.; Kapsa, P.** 2009. Identification of a friction model at tool/chip/workpiece interfaces in dry machining of AISI4142 treated steel, Journal of Materials Processing Technology, 209: 3978-3990. http://dx.doi.org/10.1016/j.jmatprotec.2008.09.019.
18. **Shaw, M.C.** 1984. Metal Cutting Principles, Oxford Science Publications, Oxford.
19. **Bahi, S.; Nouari, M.; Moufki, A.; El Mansori, M.; Molinari, A.** 2011. A new friction law for sticking and sliding contacts in machining, Tribology International 44: 764-771. http://dx.doi.org/10.1016/j.triboint.2011.01.007.
20. **Georges, J.M.** 2003. Frottement, usure et lubrification CNRS, 99-106.
21. **Sutter, G.; Ranc, N.** 2007. Temperature fields in a chip during high-speed orthogonal cutting. An experimental investigation, International Journal of Machine Tools & Manufacture 47: 1507-1517. http://dx.doi.org/10.1016/j.ijmachtools.2006.11.012.

F. Salvatore, T. Mabrouki, H. Hamdi

ANALITINIO TERMOMECHANINIO PJOVIMO MODELIO, TENKINANČIO SKAITINIUS IR EKSPERIMENTINIUS REZULTATUS, PARUOŠIMAS

R e z i u m ė

Pagrindinis šio straipsnio tikslas – pasiūlyti analitinį medžiagos pašalinimo modelį. Įvertinant visus proceso aspektus, pritaikyta „nuskėlimo“ reiškinį remianti prielaida, kai medžiagos pašalinimas yra suma trijų pagrindinių veiksnių: atplėšimo, atsispyruokliavimo ir „švaraus nupjovimo“. Ši nauja metodologija yra sukurta naudojantis eksperimentų ir gamybos patirtimi. Faktiškai drožlė ne visada susidaro. Kai drožlė susidaro, dalis pašalinamos teorinio sluoksnio medžiagos transformuojasi į užpakalinę atplaišą ir yra gniuždoma po įrankio viršūne. Straipsnyje yra pasiūlytas šis naujas požiūris ir detaliai išnagrinėta „grynojo pjovimo“ įtaka. Šis analitinis drožlės formavimosi submodelis yra kalibruotas ir pritaikytas baigtiniams elementams modeliuoti, norint pasiūlyti naują hipotezę ir naują lygybę, sukėlus fizinį reiškinį greta įrankio viršūnės. Drožlė yra standi ir vienoda, o režimas stacionarus. Termomechaninis dėsnis yra pritaikytas šlyties zonai, kur koncentruojasi plastinė deformacija, temperatūra ir deformacijos greitis. Modelis taip pat įvertina pjovimo briaunos spindulį. Naudojamas ekvivalentinis pjovimo kampas. Įrankio ir drožlės kontakte trinties koeficientas yra analitiškai apskaičiuotas ir šis modelis laikytinas prognozuojamu.

F. Salvatore, T. Mabrouki, H. Hamdi

ELABORATION OF ANALYTICAL THERMO-MECHANICAL CUTTING MODEL MATCHED BY NUMERICAL AND EXPERIMENTAL RESULTS

S u m m a r y

The global aim of this paper is to propose a complete analytical model concerning the material removal. In order to take into account all the aspects of the process, a "phenomena split approach", based on the assumption that the material removal is the summation of three major contributions, ploughing, spring back and "pure cut" was adopted. This new methodology is developed on the base of experimental tests and industrial experience. In fact the chip is not systematically present. When the chip exists, a part of theoretical layer of the material to be removed is transformed in lateral burrs and elastic compression under the tool tip. In this paper this new approach is presented and the "pure cut" contribution is developed in details. This analytical sub-model of chip formation is calibrated and fitted with a finite element modeling, in order to presents new hypothesis and new formula based on the physics close to the tip of the tool. The chip is considered rigid and uniform, and the regime is supposed stationary. Thermo-mechanical law is applied in shear zones where plastic strain, temperature and strain rate are concentrated. The model takes into account the cutting edge radius too, using an equivalent cutting angle. The friction coefficient at the interface tool-chip is also analytically computed and the present model is considered predictive.

Keywords: analytical model, thermo-mechanical cutting.

Received August 29, 2011
Accepted November 15, 2012